Available online at www.sciencedirect.com

SciVerse ScienceDirect

IERI Procedia 3 (2012) 87 – 93

Procedia IERI

www.elsevier.com/locate/procedia

2012 International Conference on Mechanical and Electronics Engineering

The Effect of Non-normality of the Navier-Stokes Operator on the Dynamics of an Axisymmetric Swirling Flow

Chen Cheng[1*]

[1]*Low Speed Aerodynamics Institute, China Aerodynamics Research and Development Center, Mianyang, Sichuan 622762, China;*

Abstract

We consider in detail the effect of non-normality of the Navier-Stokes operator on the time evolution of an axisymmetric swirling flow. The eigenvalue analysis and transient growth analysis have been employed to obtain the least stable eigenmode and the global optimal perturbation respectively, which are both taken as the initial disturbances. Three stages of dynamic process have been observed for the dynamics of the optimal perturbation. In the linear stage the result of the amplification of perturbation energy is consistent with that revealed by transient growth theory. Having come into the nonlinear stage, the perturbation energy growth is suppressed by the interaction with the Oseen vortex core. Finally, the phenomena of secondary energy growth is also observed. Compared with the results obtained by applying the least stable eigenmode as the initial disturbance, the nonlinear behavior of the optimal perturbation features radial fluid motion and the rapid production of small eddies. The effect of perturbation amplitude on the nonlinear evolution of flows is also investigated.

*Keywords:*Swirling flow, global optimal perturbation, time evolution

Swirling flows are commonly encountered in many situations of interest, e.g., in mixing and combustion problems, and their stability properties have received considerable attention in recent years. Early researches about linear stability analysis were focused on the normal mode method,, for which many types of instability mechanisms are now well stuided, i.e. the centrifugal instability [1], the elliptical instability [2], and so on. The present work is mainly devoted to the evolution of small perturbations in the Oseen vortex, which has the azimuthal velocity

$$V = (1 - e^{-r^2}) / r, \qquad (1)$$

where r is the radial coordinate. According to the results of linear stability analysis [3], the Oseen vortex, not subjected to any external strain, is normal-mode stable..

However, normal-mode stability does not imply perturbations can not grow because of the non-normality in the linearized Navier-Stokes operator. That is, perturbations formed from superposition of non-orthogonal eigenfuctions may experience large growth even when every composing eigenfunction corresponds to a negative growth rate. This phenomena of energy amplification, named as transient growth, may be associated with subcritical transition in parallel shear flows [4-5]. More recently, transient growth analysis has also been applied to swirling flows widely [6-8].

The present knowledge about the transient growth characteristics of the Oseen vortex [8] leads naturally to the question of what is the nonlinear behavior of the optimal perturbation, and whether the flow evolves to self-sustaining turbulence.

 doi:10.1016/j.ieri.2012.09.015

The objective of the article is to investigate these questions via direct numerical simulation, as is the case for the dynamics of a laminar separation bubble [9]. In this study, our computations are limited to axisymmetric cases.

1. Numerical implemetation

1.1. Finite difference scheme

We adopt the finite-difference scheme in cylindrical coordinates [10] for the direct simulation of the incompressible time-dependent Navier–Stokes equations. The computational domain is denoted as $\mathbf{R}=\{(r,z)\,|\,0\le r\le R_{\max},0\le z\le L_{\max}\}$, where the axial length $L_{\max}$ is the wavelength of disturbance. The free-slip condition is used at the radial boundary $r=R_{\max}$.

1.2. Initial conditions

For fixed Re and axial wavenumber k, the global optimal perturbation, which achieves the maximum value of the gain curve $G(t)$, and its energy growth curve $E(t)$ can be derived by transient growth computation. The transient growth problem is solved through a standard methodology described in [11]. Similarly, the normal eigenmodes are obtained from classical linear stability analysis. In the following, the initial perturbation $\mathbf{u}(r,z,0)$ is of the form

$$\varepsilon([\tilde{u}_\theta(r),\tilde{u}_r(r),\tilde{u}_z(r)]e^{ikz}+c.c.), \tag{2}$$

where $\tilde{u}_\theta(r)$, $\tilde{u}_r(r)$ and $\tilde{u}_z(r)$ are the azimuthal, radial, and axial velocities of the global optimal perturbation or the least stable eigenmode，and ε the proportional coefficient.

The two types of perturbations are depicted in Fig. 1 for a representative simulation $(\mathrm{Re}=5000,k=\pi)$, which is featured by significant transient growth. At this set of parameters, the global optimal energy growth function G_O equals to 344.6. Clearly, the perturbation vorticity distribution of the global optimal perturbation outside the core is relatively oscillatory in r. In contrast to this, the azimuthal vorticity field for the least stable eigenmode is localized within the vortex core.

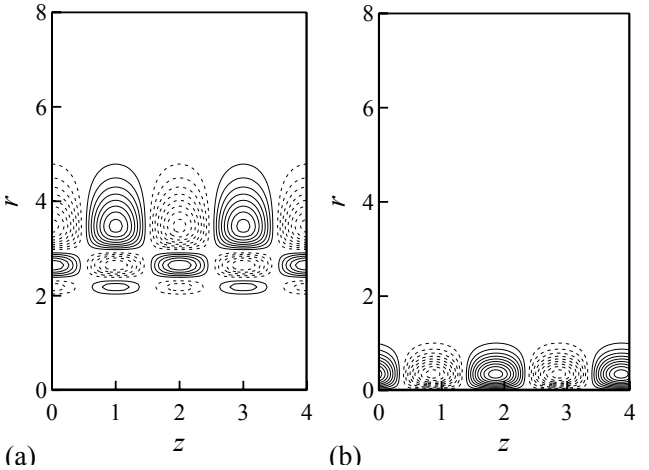

Fig. 1 The contours of azimuthal vorticity fields corresponding to the two types of initial perturbations for Re=5000, k=π. (a) The global optimal perturbation. (b) The least stable eigenmode.

2. Results and discussions

In the following, we will first discuss the results for the set of parameters mentioned above with a gird of 256×64 in (r,z) directions. Fig. 2 shows the variation of perturbation energy with time for the optimal perturbation and the least stable eigenmode, respectively. The perturbation amplitude ε is set to be 0.03. As seen in the $E\sim t$ curve for the optimal perturbation, we roughly divide the dynamic process of the axisymmetric flow into three stages: (1) energy linear growth; (2) energy decay due to nonlinear interaction; (3) secondary energy growth.

2.1. Typical results

Fig. 3 shows the azimuthal vorticity contours during the early evolution of the optimal perturbation, which grows linearly until $t \approx 35$ and reaches saturation at $t \approx 75$ subsequently, as seen in Fig. 2(a). Moreover, during the early period, the $E \sim t$ curve is nearly coincident with the one derived by transient growth analysis, implying that the initial stage of evolution is assuredly dominated by the non-normality of the linearized Navier-Stokes operator. The vortex ring shape remains almost unchanged (Fig. 3). With time, the energies in radial and axial components grow rapidly. Meanwhile, the azimuthal energy decreases over a short period of time until the eventual growth starts (Fig. 4). This observation is consistent with the so-called anti-lift-up mechanism [12]. Note that the radial perturbation is quite larger than other directions in magnitude, similar as the azimuthal vorticity.

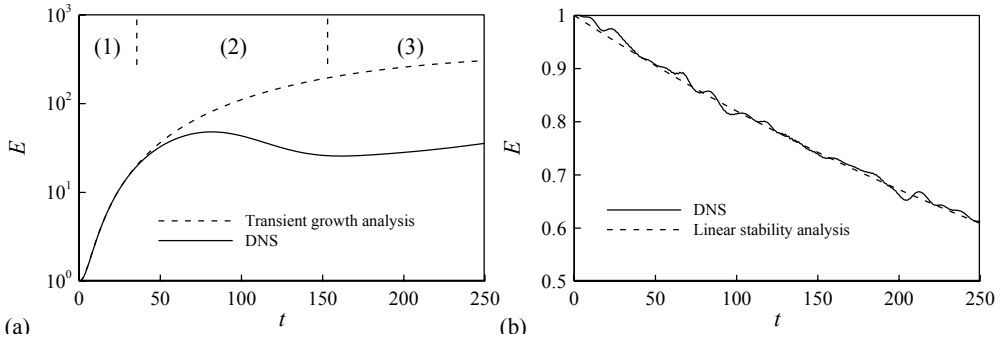

Fig. 2 Perturbation energy evolution of the optimal perturbation (a) and the least stable eigenmode (b) with time for Re=5000, k=π.

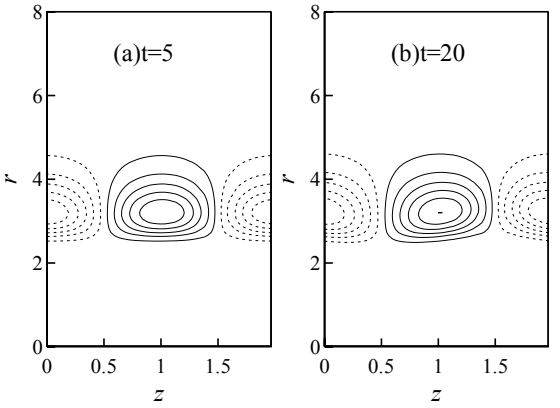

Fig. 3 Contours of azimuthal vorticity for early evolution of the optimal perturbation with Re=5000, k=π. The maximum value, minimum value, and the increment are (a) 0.0244, -0.0244, 0.0045; (b) 0.0942, -0.0942.

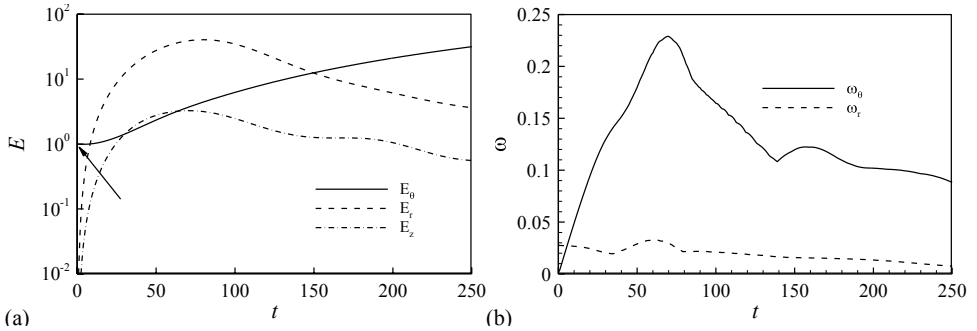

Fig. 4 The time evolution of the kinetic energies in all the three directions (a) and the vorticity maximum in the azimuthal and axial directions (b) for the optimal perturbation, Re=5000, k=π.

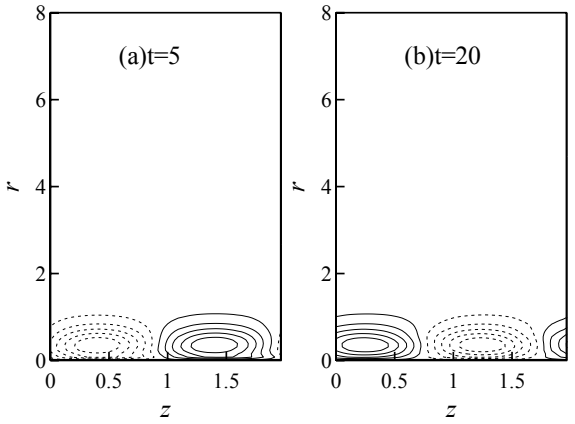

Fig. 5 Azimuthal vorticity contours for early evolution of the least stable eigenmode perturbation. The maximum value, minimum value, and the increment are (a) 0.0358, -0.0365, 0.0065; (b) 0.0342, -0.0347, 0.0063.

Fig. 5 presents the early evolution of azimuthal vorticity contours for the least stable eigenmode. In contrast to the case of the global optimal perturbation, the perturbation energy always decreases with time for the least stable eigenmode, being consistent with the growth rate results obtained from linear stability analysis (Fig. 2b). Moreover, the perturbation field is always limited in the vortex core region. The results imply that in a normal-mode-stable flow, the linear growth process due to the non-normality is necessary for rich dynamic phenomena of nonlinear evolution.

During $t = 75 - 150$, the perturbation energy decreases as time increases (Fig. 2a). It seems to be the strong interaction between the vortex ring formed from the optimal perturbation outside and columnar vortex core that generate a relative oscillatory radial distribution of azimuthal vorticity (fig. 6a~b). Meanwhile, all the velocity components are also decreased and the location of the maximum vorticity is shown to move radially outward. As shown in Fig. 6c, a pair of vortex rings with opposite sign moves radially and transports fluid outward from the vortex core region, alike the case of a swirling jet found by Hu et al. [13]. They suggested this radial motion of fluid is favorable to fluid mixing. Herein, we conclude that the similar results can also be obtained by applying the optimal perturbation as the initial condition, rather than a single eigenmode. Note that the flow characteristics of the least stable eigenmode in this stage are similar as those in the energy growth stage, and we don not show them herein for briefness.

With increasing time, the azimuthal vorticity field with a oscillatory radial distribution interacts with the Oseen vorterx, leading to durative drop of perturbation velocities. Thus, the velocity field has a increasing difference with the basic azimuthal velocity profile, leading to the growth of perturbation energy (Fig. 2a). As seen in Fig. 6e, the radial motion of a pair of azimuthal vortex rings with opposite sign is observed again, though the magnitude of vorticity is quite less than that seen in the stage of energy decay. At $t = 900$, three arrays of vorices lie in a large radial location. Note that another effect of the optimal perturbation is the rapid production of small eddies, see e.g. fig. 6e, which is thought to be another possible mechanism for enhancement for fluid mixing.

2.2. Influences of parameters on flow evolution

Here we aim to study the effects of the Reynolds number Re and the axial wavenumber k on the time evolution of axisymmetric flows.

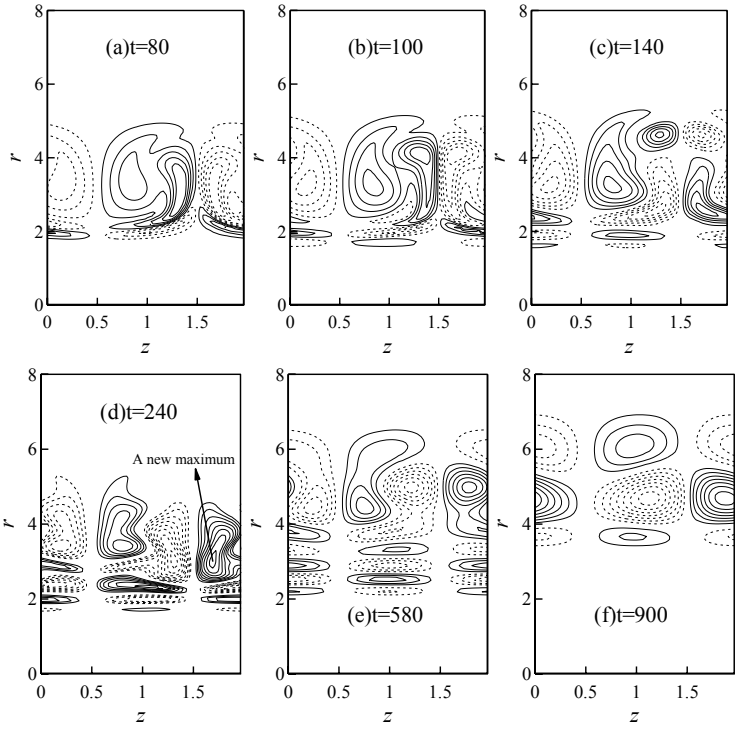

Fig. 6 Azimuthal vorticity contours for $t > 75$ with Re=5000, k=π. The maximum value, minimum value, and the increment are (a) 0.207, -0.207, 0.038; (b) 0.165, -0.165, 0.03; (c) 0.1, -0.1, 0.02; (d) 0.09, -0.095, 0.01; (e) 0.012, -0.012, 0.002; (f) 0.077, -0.007, 0.001.

In the following, we introduce two quantities of time T_1 and T_2, denoting the lengths of the linear growth stage and the perturbation energy decay stage, respectively. The variation of T_1 and T_2 with k for $\mathrm{Re} = 5000$ is shown in Fig. 7a. With increasing k, both T_1 and T_2 decrease monotonously. This would imply that larger values of k lead to stronger viscous dissipation and smaller T_1 and T_2; smaller values of k lead to weaker viscous dissipation and larger T_1 and T_2. Similarly, the fact that T_1 and T_2 increases with increasing Re, as seen in Fig. 7b, can also be explained in terms of viscous dissipation.

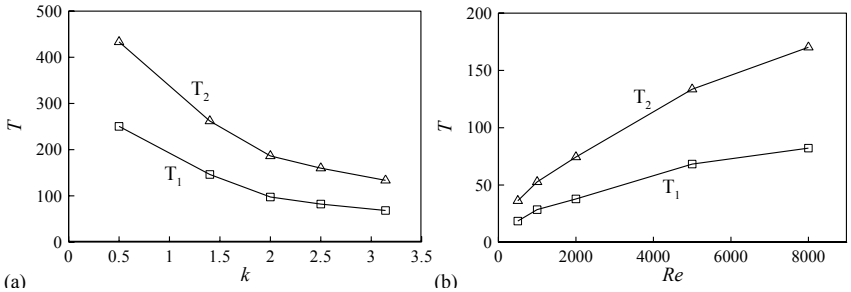

Fig. 7 The variation of T_1 and T_2 with the axial wavenumber k and the Reynolds number Re. (a) Re=5000,. (b) k=π.

2.3. The choice of perturbation amplitude

As mentioned above, some phenomena which are beneficial to fluid entrainment will appear at the nonlinear evolution stage of the optimal perturbation when an appropriate value of perturbation amplitude is chosen. Thus, it is natural to raise an interesting question of how to choose the amplitude value.

Fig. 8 plots the evolution of azimuthal vorticity field with a quite small amplitude $\varepsilon = 0.001$, other parameters are the same as for Fig. 2. Clearly, with increasing time, there is little change in perturbation structure when coming into the nonlinear stage (Fig. 8c~d). Besides, the evolution behaviors, such as the radial motion of fluid, are not observed again. These results would imply that the magnitude of the perturbation amplitude has a key impact on the nonlinear behaviors of a

normal-mode-stable flow with significant transient growth. When this value is relatively small, flow nonlinear evolution is similar to that for the least stable eigenmode; when it is relatively large, some issues are found to be responsible for mixing enhancement.

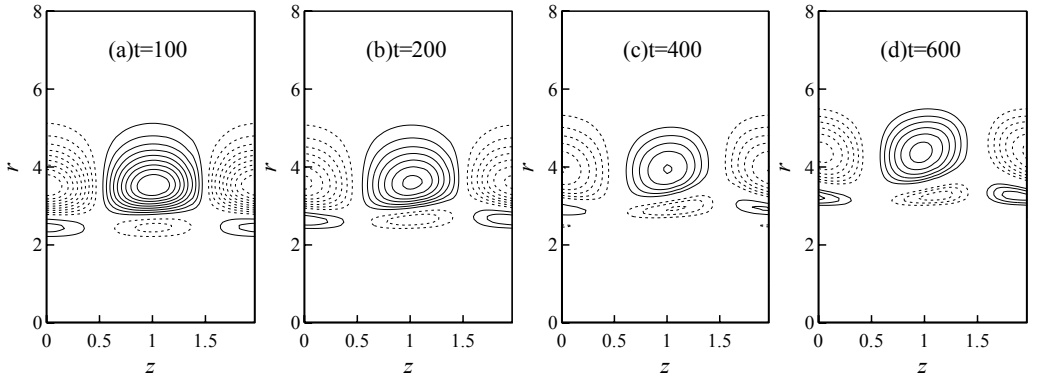

Fig. 8 Azimuthal vorticity contours for evolution of the optimal perturbation with ε=0.001. The maximum value, minimum value, and the increment are (a) 0.009, -0.009, 0.001; (b) 0.014, -0.014, 0.002; (c) 0.012, -0.012, 0.002; (d) 0.007, -0.007, 0.001.

Having examined the dynamics of the optimal perturbation with large transient growth, we now turn to one case with relatively small energy transient growth. The variation of azimuthal vorticity contours with time is shown in Fig. 9 with $\mathrm{Re}=318, k=\pi$. For this particular case, $G_O=4.80$. Clearly, the nonlinear evolution behaviors, such as the outward radial motion, are absent for both the large perturbation amplitude $\varepsilon=0.05$ and the small one $\varepsilon=0.001$. The result would imply that for cases with small energy transient growth, large perturbation amplitude ($\varepsilon=0.05$) is not sufficient to induce the nonlinear evolution behaviors yet. According to this conclusion, combined with the discussion of the large transient growth case, it seems that the full development of the initial perturbation at the linear growth stage is essential for the appearance of nonlinear evolution behaviors which enhance fluid mixing. For the large transient growth case with a quite small perturbation coefficient ($\varepsilon=0.001$), the optimal perturbation does not grow up to an enough level, and thus it cannot induce those nonlinear evolution behaviors; for the case with small transient growth ($\mathrm{Re}=318, k=\pi$), the situations are similar.

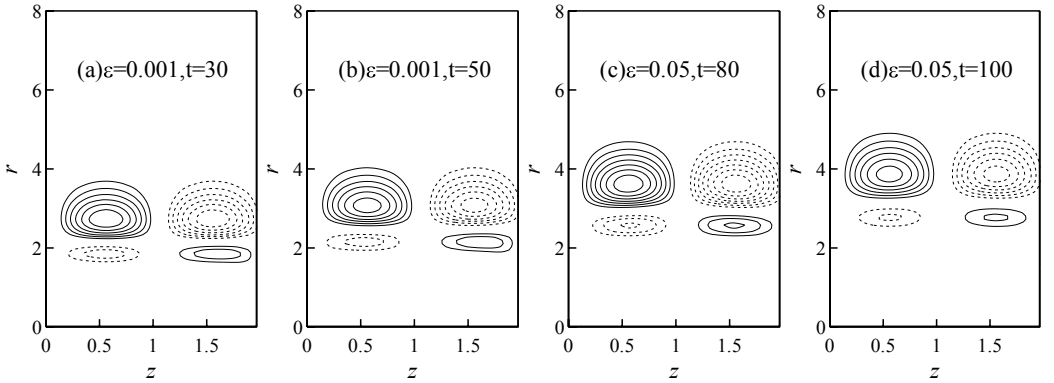

Fig. 9 Azimuthal vorticity contours for evolution of the optimal perturbation with $\mathrm{Re}=318, k=\pi$. The maximum value, minimum value, and the increment are (a) 0.0014, -0.0014, 0.0002; (b) 0.0007, -0.0007, 0.0001; (c) 0.008, -0.008, 0.001; (d) 0.0035, -0.0035, 0.0005.

3. Comclusions

We have conducted a numerical simulation for the time evolution of a swirling flow. In axisymmetric cases, the evolution process of the optimal perturbation could be divided into three stages. After the stage of energy linear growth, the vortex ring, which experiences a full development, interacts with the columnar vortex in the core region, leading to the arrest of the perturbation energy growth. Meanwhile, the radial motion of a vortex pair is observed. With increasing time, the energy of the optimal perturbation increases again, and small eddies are seen to appear in the flow field. This observation combined with the radial motion of fluid are thought to be favorable to fluid mixing.

In contrast to the case of the optimal perturbation, the perturbation field of the least stable eigenmode is always limited in the vortex core, and its magnitude decreases with time. The observations, combined with the results for the optimal perturbation, indicate that the transient growth process is necessary for rich dynamic phenomena mentioned above, which enhances fluid mixing.

The discussion on the perturbation amplitude shows that the initial perturbation has to be amplified to a fully large level at the linear growth stage to induce the nonlinear evolution behaviors. Otherwise, as for the large transient growth case with $\varepsilon = 0.001$, those behaviors can not appear yet.

References

[1] Sreedhar M, Ragab S. Large eddy simulation of longitudinal stationary vortices. Phys Fluids, 1994, 6: 2501-2514
[2] Kerswell R R. Elliptical instability. Annu. Rev. Fluid Mech., 2002, 34: 83-113
[3] Lessen M R, Singh P J, Paillet F. The stability of a trailing line vortex. Part 1. Inviscid theory, J. Fluid Mech., 1974, 63: 753-763
[4] Gustavsson L H. Energy growth of three-dimensional disturbances in plane Poiseuille flow. J. Fluid Mech., 1991, 224: 241-260
[5] Butler K M, Farrell B F. Three-dimensional optimal perturbations in viscous shear flow. Phys Fluids, 1992, A4(8): 1637-1650
[6] Heaton C J Optimal growth of the Batchlor vortex viscous modes, J. Fluid Mech., 2007, 592: 495-505
[7] Heaton C J. Optimal linear growth in sprial Poiseuille flow, J. Fluid Mech., 2008, 607: 141-165
[8] Pradeep D S, Hussain F. Transient growth of perturbations in a vortex column, J. Fluid Mech., 2006, 550: 251-288
[9] Cherubini S, Robinet J C, Palma P D. The effects of non-normality and nonlinearity of the Navier-Stokes operator on the dynamics of a large laminar separation bubble, Phys Fluids, 2010, 22: 014102
[10] Verzicco R, Orlandi P. A finite difference scheme for the three dimensional impressible flows in cylindrical coordinates, J. Comput. Phys., 1996, 123: 402-414
[11] Schmid P J, Henningson D S. Stability and Transition in Shear Flows (Springer-Verlag, New York, 2001)
[12] Antkowiak A. Dynamique aux temps courts d'un tourbillon isole. PhD thesis, Universite Paul Sabatier, Toulouse, France, 2005
[13] Hu G H, Sun D J, Yin X Y. A numerical study of dynamics of a temporally evolving swirling jet, Phys Fluids, 2001, 13(4): 951-965